Surface rotation and magnetic activity for 55,000+ *Kepler* solar-type stars

Ângela R. G. Santos, S. N. Breton, Savita Mathur, Rafael A. García

WARWICK THE UNIVERSITY OF WARWICK

✉ angela.goncalves-dos-santos@warwick.ac.uk

Abstract

Spots lead to brightness variations that enclose details on stellar rotation and magnetic activity. We analyzed *Kepler* data of 159,710 main-sequence and subgiant FGKM stars. We recover rotation periods P_{rot} and photometric activity proxy S_{ph} for 55,201 stars, which corresponds to a detection increase of $\sim 60\%$ in comparison with McQuillan et al. (2014, McQ14). In particular, we report a larger number of slow rotators, shifting the upper edged of the P_{rot} distribution towards longer P_{rot}.

Target sample and data preparation

- ⋆ DR25: cross-check (Mathur et al. 2017)
- ⋆ B20: reference stellar properties (Berger et al. 2020)
- ⋆ subsample I: main-sequence and subgiant FGKM stars in DR25 & B20 (Santos et al. 2019, Santos et al. in prep.)
- ⋆ subsample II: main-sequence or subgiant FGK stars only in DR25 or B20
- ⋆ 3 KEPSEISMIC lightcurves†: 20-d, 55-d, and 80-d filter (García et al. 2011)
- ⋆ PDC-MAP lightcurves (Jenkins et al. 2010)
- ⋆ Identifying known and candidate contaminants (classical pulsators, red giants, close-in binaries, ...)

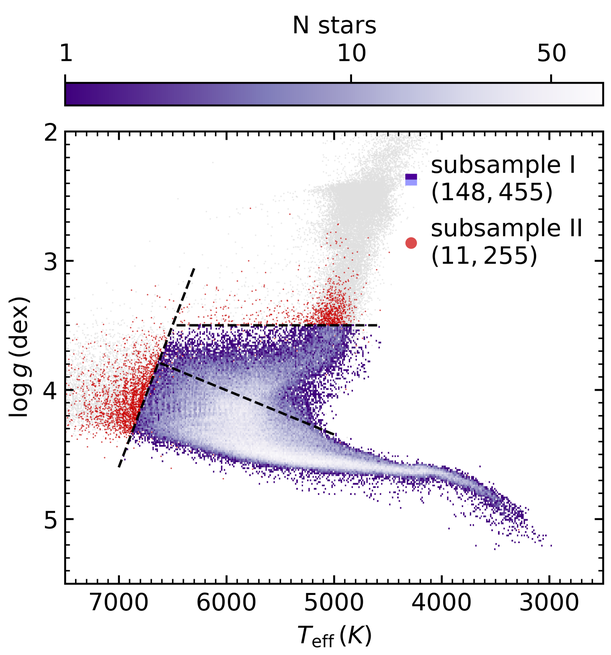

Rotation and photometric activity

- ⋆ Rotation period candidates for each lightcurve (Mathur et al. 2010; García et al. 2014; Ceillier et al. 2016, 2017; Santos et al. 2019)
  - ∗ global wavelet spectrum ∗ autocorrelation function ∗ composite spectrum
- ⋆ Final P_{rot}
  - ∗ machine learning (ROOSTER; Breton et al. 2021)
  - ∗ automatic selection (P_{rot}-candidate agreement; peak-height treshold)
  - ∗ additional visual inspection
- ⋆ photometric activity proxy S_{ph} (Mathur et al. 2014)

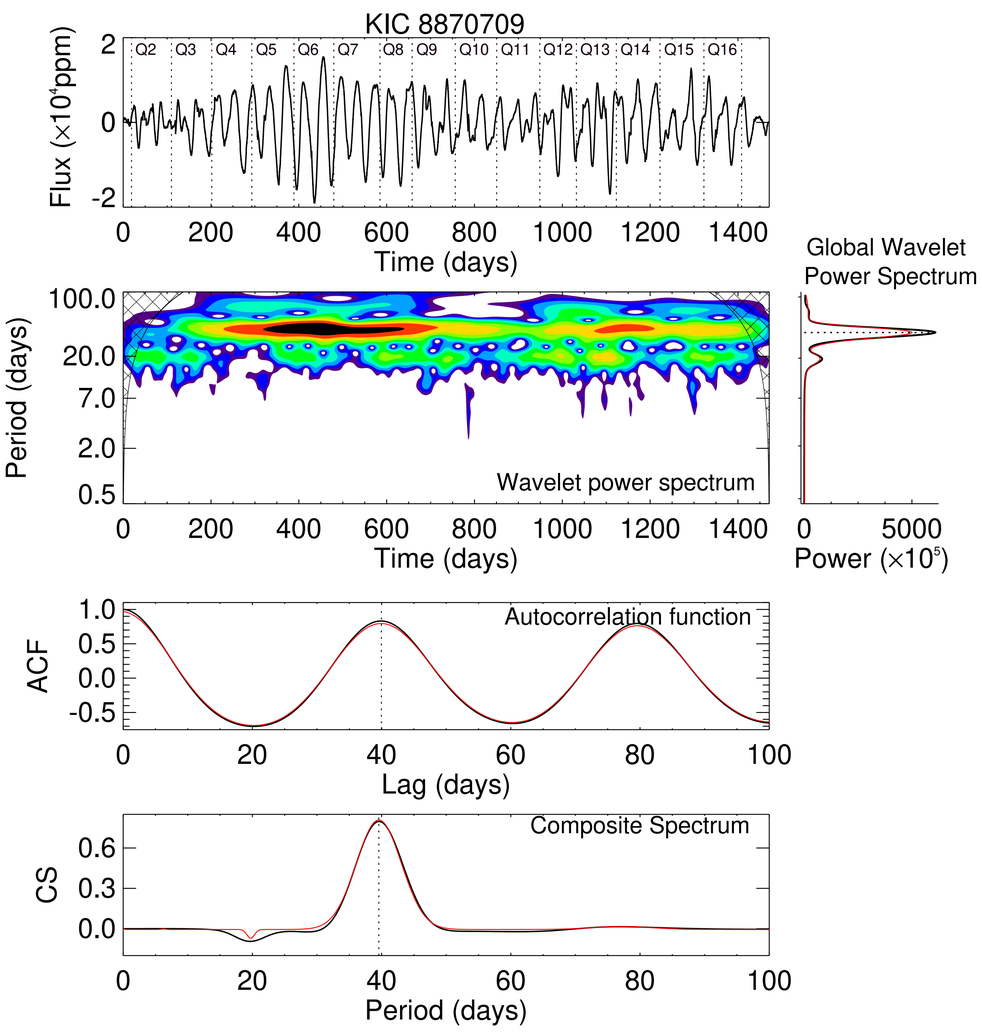

Ensemble Results

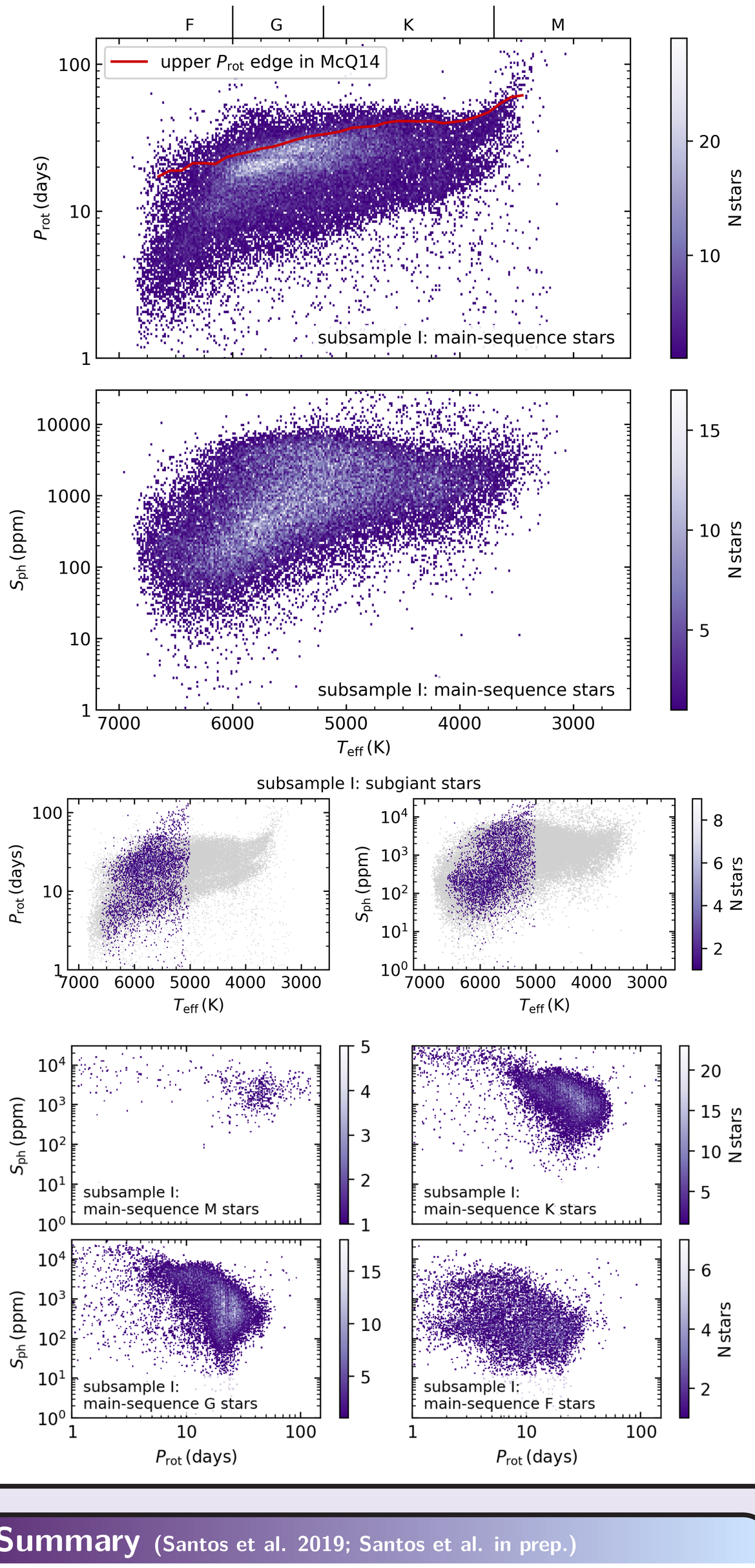

Summary (Santos et al. 2019; Santos et al. in prep.)

		with P_{rot}	without P_{rot}	detection fraction
Subsample I	main-sequence M stars	801	560	58.9%
	main-sequence K stars	17,441	11,005	61.3%
	main-sequence G stars	19,430	42,332	31.5%
	main-sequence F stars	9,446	22,982	29.1%
	subgiant stars	4,692	18,150	20.5%
	Subsample II	2,790	6,520	29.9%
	Subsample III	601	1,344	30.9%
	Total	55,201	102,945	53.6%

†KEPSEISMIC data on MAST: https://doi.org/10.17909/t9-mrpw-gc07

Acknowledgements: SSI; STFC grant ST/T000252/1SFCT; NASA grant NNX17AF27G; PLATO & GOLF CNES grants; Spanish ministry grant RYC-2015-17679

References:
Berger, T. A., et al. 2020, AJ, 159, 280
Breton, S. N., et al. 2021, arXiv:2101.10152
Ceillier, T., et al. 2017, A&A, 605, A111
Ceillier, T., et al. 2016, MNRAS, 456, 119
García, R. A., et al. 2014, A&A, 572, A34
García, R. A., et al. 2011, MNRAS, 414, L6
Jenkins, J. M., et al. 2010, ApJL, 713, L87
Mathur, S., et al. 2014, A&A, 562, A124
Mathur, S., et al. 2010, A&A, 518, A53
Mathur, S., et al. 2017, ApJS, 229, 30
McQuillan, A., et al. 2014, ApJS, 211, 24
Santos, A. R. G., et al. 2019, ApJS, 244, 21